DIAGRAM ANALYSIS OF THE HUBBARD MODEL: STATIONARITY PROPERTY OF THE THERMODYNAMIC POTENTIAL

V. A. Moskalenko^{a,b*}, **L. A. Dohotaru**^{c**}, **I. D. Cebotari**^{a}

^{a}*Institute of Applied Physics, Moldova Academy of Sciences*
2028, Chisinau, Moldova

^{b}*Joint Institute for Nuclear Research*
141980, Dubna, Russia

^{c}*Technical University*
2004, Chisinau, Moldova

The diagram approach proposed many years ago for the strongly correlated Hubbard model is developed with the aim to analyze the thermodynamic potential properties. A new exact relation between renormalized quantities such as the thermodynamic potential, the one-particle propagator, and the correlation function is established. This relation contains an additional integration of the one-particle propagator with respect to an auxiliary constant. The vacuum skeleton diagrams constructed from the irreducible Green's functions and tunneling propagator lines are determined and a special functional is introduced. The properties of this functional are investigated and its relation to the thermodynamic potential is established. The stationarity property of this functional with respect to first-order variations of the correlation function is demonstrated; as a consequence, the stationarity property of the thermodynamic potential is proved.

1. INTRODUCTION

The Hubbard model is one of the most important models for electrons in solids; it describes quantum mechanical hopping of electrons over lattice sites and their short-range repulsive Coulomb interaction. This model was discussed by Hubbard [1] in describing a narrow-band system of transition metals; it has been revised to investigate the properties of highly correlated electron systems such as copper oxide superconductors.

The Hubbard model exhibits various phenomena including a metal–insulator transition, antiferromagnetism, ferromagnetism, and superconductivity. This model assumes that each atom of the crystal lattice has only one electron orbit and the corresponding orbital state is nondegenerate.

The Hamiltonian of the Hubbard model is a sum of two terms,

$$H = H^0 + H', \qquad (1)$$

where H^0 is the atomic contribution, which contains the Coulomb interaction term U and the local electron energy $\overline{\epsilon}$ in the atom

$$H^0 = \sum_{\mathbf{i}} H_{\mathbf{i}}^0,$$
$$H_{\mathbf{i}}^0 = \sum_{\sigma} \epsilon n_{\mathbf{i}\sigma} + U n_{\mathbf{i}\uparrow} n_{\mathbf{i}\downarrow}, \qquad (2)$$
$$\epsilon = \overline{\epsilon} - \mu, \quad n_{\mathbf{i}\sigma} = C_{\mathbf{i}\sigma}^{\dagger} C_{\mathbf{i}\sigma},$$

μ is the chemical potential, H' is the hopping Hamiltonian,

$$H' = \sum_{\mathbf{i},\mathbf{j}} \sum_{\sigma} t(\mathbf{i}-\mathbf{j}) C_{\mathbf{i}\sigma}^{\dagger} C_{\mathbf{j}\sigma},$$
$$t(\mathbf{i}-\mathbf{j}) = t^*(\mathbf{j}-\mathbf{i}), \quad t(\mathbf{0}) = 0, \qquad (3)$$

$C_{\mathbf{i}\sigma}^{\dagger}$ ($C_{\mathbf{i}\sigma}$) are the creation (annihilation) electron operators at a local site $\mathbf{i}$ and with spin σ, and t is the hopping integral. In the thermodynamic perturbation theory, we use thermal averages in a grand canonical

---

*E-mail: moskalen@theor.jinr.ru
**E-mail: statphys@asm.md

ensemble, and therefore the term $-\mu \hat{N}_e$, with the electron number operator

$$\hat{N}_e = \sum_{\mathbf{i},\sigma} n_{\mathbf{i}\sigma}, \qquad (4)$$

is added to Hamiltonian (1). The quantities U and $\hat{N}_e$ are the fundamental parameters of the model. The large Coulomb repulsion is taken into account in the zeroth approximation of our theory. The operator H', which describes hopping of the electrons between sites of the crystal lattice, is regarded as a perturbation.

New physical and mathematical concepts and techniques have been elaborated for investigating this model. We can only mention some of them. There are many analytic approximations such as the Hubbard approximation, the noncrossing approximation, the slave-boson method, dynamical mean field theory, and composite and other projection operator methods and approaches.

Numerical simulations of thermodynamic quantities and the density of states have also been performed by various methods. Some exact results for the one- and two-dimensional Hubbard model are known. Each approximate method has its advantages and disadvantages. A short and comprehensive review of the methods can be found in papers and books [2–7]. In addition to these approaches, we also mention the special diagram techniques elaborated for strongly correlated electron systems. In Refs. [8–10], a diagram technique for the Hubbard model was developed based on disentangling the nondiagonal Hubbard operator from time-ordered products of other such operators. Because the algebra of the Hubbard transfer operators is more complicated than that of Fermi operators, the essential features of this technique remain poorly developed.

Other diagram approaches around the atomic limit have also been proposed for the Hubbard model in both normal [11,12] and superconducting [13] states. The theory introduces the generalized Wick theorem (GWT) that uses a cumulant expansion of the statistical average values for the products of fermion operators. The GWT takes into account the fact that the Hamiltonian H^0 is nonquadratic in fermion operators due to the Coulomb interaction. This last circumstance is responsible for the appearance of the nonvanishing site cumulants called the irreducible Green's functions. These new Green's functions take all the spin, charge, and pairing fluctuations of the system into account. The perturbation formalism around the atomic limit has the advantage that local (atomic) physical properties can be evaluated exactly and the transfer of this local information to neighboring sites due to kinetic

mobility of the conduction electrons can be handled perturbatively in powers of the hopping integral.

A GWT for chronological averages of products of electron operators was subsequently formulated also by Metzner [14]. Metzner did not derive a Dyson-type equation for the renormalized one-particle Green's function, and the role of our correlation function was not established. In spite of the similarity to our works, the diagrams in his approach are quite different from ours. The n-particle cumulant is represented by a $2n$-valent-point vertex with n incoming and n outgoing lines, whereas in our approach, such a cumulant or irreducible Green's functions is represented by a rectangle with $2n$ vertices with n incoming and n outgoing arrows. The rectangle contains vertices with the same site index but different time and spin labels. In addition, Metzner investigated the limit of high lattice dimensions.

In this paper, we develop the diagram theory proposed previously for the Hubbard model [11, 12] with the aim to demonstrate the existence of a relation between renormalized values of the thermodynamic potential and the one-particle Green's function and also to prove the stationarity properties of this potential. Such a theorem was first proved by Luttinger and Ward [15] for uncorrelated systems by using the diagram technique of weak-coupling field theory.

The strong-coupling diagram theory used by us requires new concepts and new equations to prove the stationarity properties of the thermodynamic potential for strongly correlated systems. Such a proof has already been achieved for the Anderson impurity model in [16].

This paper is organized as follows. In Sec. 2, we develop the diagram theory in the strong-coupling limit and introduce the skeleton diagrams. In Sec. 3, we prove the stationarity theorem for the renormalized thermodynamic potential. Section 4 contains our conclusions.

2. PERTURBATIVE TREATMENT

We use the definition of the one-particle Matsubara Green's functions in the interaction representation as in [11, 12],

$$G(x|x') = - \left\langle TC_{\mathbf{x}\sigma}(\tau)\overline{C}_{\mathbf{x}'\sigma'}(\tau')U(\beta) \right\rangle_0^c, \qquad (5)$$

where x stands for $(\mathbf{x}, \sigma, \tau)$ and the superscript "c" denotes the connected part of the diagrams that appear in the right-hand side of Eq. (5). We use a somewhat generalized series expansion for the evolution operator
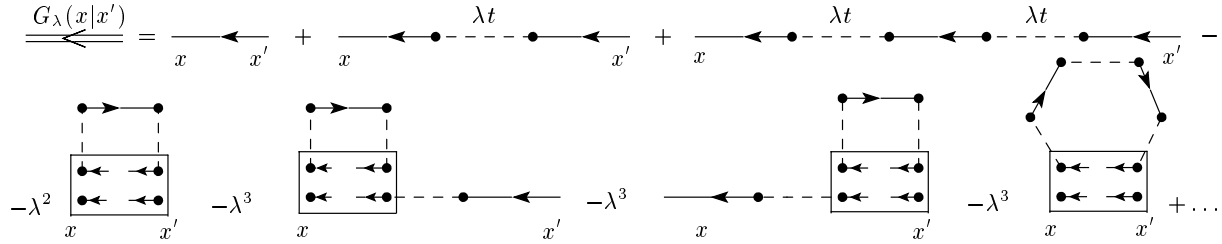
Fig. 1. First three orders of the perturbation theory for the one-particle propagator. The solid line depicts the zeroth-order propagator and the dashed line depicts the tunneling matrix element. The rectangles depict irreducible two-particles Green's functions $G_2^{(0)ir}$, and dots are the vertices of the diagrams

$U(\beta)$ because we introduce an auxiliary constant λ and use $\lambda H'$ instead of H':

$$U_\lambda(\beta) = T \exp\left(-\lambda \int_0^\beta H'(\tau)\, d\tau\right). \qquad (6)$$

In the presence of this constant, we use λ as a label for all dynamic quantities such as $G_\lambda(x|x')$. At the final stage of the calculations, this constant it set equal to unity.

In the zeroth-order approximation, the one-particle Green's function $G^{(0)}(x|x')$ is local,

$$G^{(0)}(x|x') = \delta_{\mathbf{x}\mathbf{x}'}\delta_{\sigma\sigma'}G^{(0)}(\tau - \tau'), \qquad (7)$$

and its Fourier representation is

$$
\begin{aligned}
G_\sigma^{(0)}(i\omega_n) &= \int_0^\beta G_\sigma^{(0)}(\tau)\exp(i\omega_n\tau)\, d\tau = \\
&= \frac{1}{Z_0}\left(\frac{\exp(-\beta E_0) + \exp(-\beta E_\sigma)}{i\omega_n + E_0 - E_\sigma} + \right. \\
&\quad \left. + \frac{\exp(-\beta E_{\overline{\sigma}}) + \exp(-\beta E_2)}{i\omega_n + E_{\overline{\sigma}} - E_2}\right), \quad (8)
\end{aligned}
$$

where

$$
\begin{aligned}
Z_0 = \exp(-\beta E_0) + \exp(-\beta E_\sigma) + \\
+ \exp(-\beta E_{\overline{\sigma}}) + \exp(-\beta E_2),
\end{aligned}
$$

$$E_0 = 0, \quad E_\sigma = E_{\overline{\sigma}} = \epsilon, \quad E_2 = 2\epsilon + U,$$

$$\overline{\sigma} = -\sigma, \quad \omega_n = (2n+1)\pi/\beta,$$

with E_0, E_σ, and E_2 being the energies of atomic sites.

As was proved in [11, 12], propagator (5) has the diagram representation depicted in Fig. 1. The order-n irreducible Green's functions are shown with rectangles with $2n$ vertices. The arrows entering a vertex denote annihilated electrons, and those that go out, created electrons.
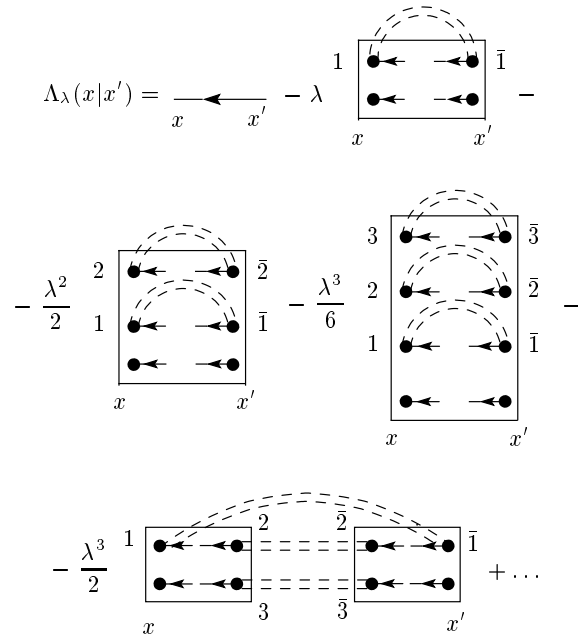
Fig. 2. Skeleton diagrams for the correlation function Λ_λ. Double dashed lines depict the tunneling Green's functions T_λ and rectangles depict the irreducible Green's functions

In [11], we introduced the notion of a correlation function $Z_\lambda(x|x')$ that is the sum of strongly connected diagrams containing irreducible Green's functions and is related to the more convenient function

$$\Lambda_\lambda(x|x') = G^0(x|x') + Z_\lambda(x|x').$$

In Fig. 1, the fourth and seventh diagrams in the right-hand side pertain to the correlation function. Because irreducible functions are local and tunneling matrix elements have the property that $t(\mathbf{x} - \mathbf{x}) = 0$, all the diagrams containing self-locked tunneling elements are omitted in Fig. 1.

As can be seen from Fig. 1, the process of propagator renormalization is accompanied by an analogous renormalization process for tunneling matrix elements and by the replacement of the instantaneous quantity

$$\lambda t(x - x') = \lambda t(\mathbf{x} - \mathbf{x}')\delta(\tau - \tau' - 0^+)$$

with the dynamical one

$$\widetilde{T}_\lambda(x|x') = \lambda t(\mathbf{x} - \mathbf{x}')\delta(\tau - \tau' - 0^+) + \\ + \sum_{1,2} \lambda t(x - 1)G_\lambda(1|2)\lambda t(2 - x'), \quad (9)$$

which in the Fourier representation

$$t(\mathbf{x}) = \frac{1}{N}\sum_{\mathbf{k}} \epsilon(\mathbf{k})\exp(-i\mathbf{k}\cdot\mathbf{x}),$$

$$G_\lambda(x|x') = \frac{1}{N}\sum_{\mathbf{k}} \frac{1}{\beta}\sum_{\omega_n} G_\lambda(\mathbf{k}|i\omega_n) \times \\ \times \exp[-i\mathbf{k}\cdot(\mathbf{x} - \mathbf{x}') - i\omega_n(\tau - \tau')]$$

becomes

$$\widetilde{T}_\lambda(\mathbf{k}|i\omega_n) \equiv \lambda T_\lambda(\mathbf{k}|i\omega_n) = \\ = \lambda\epsilon(\mathbf{k})[1 + \lambda\epsilon(\mathbf{k})G_\lambda(\mathbf{k}|i\omega_n)]. \quad (10)$$

The renormalized tunneling matrix element T_λ is in fact the tunneling Green's function and is to be depicted as a double dashed line (see Fig. 2). The matrix element $\widetilde{T}_\lambda$ is represented by such a double dashed line times λ.

We now introduce the skeleton diagrams that contain only the irreducible Green's functions and dashed lines without any renormalization. In such skeleton diagrams, simple dashed lines are replaced with double dashed lines, with the complete renormalization of dynamical quantities.

The skeleton diagrams for the correlation function Λ_λ are shown in Fig. 2. They are of two kinds. The first four diagrams are local and therefore their Fourier representation is independent of the momentum. The last diagram and others with more rectangles are not local and their Fourier representation depends on the momentum. Only the first category of diagrams are taken into account in dynamical mean field theory.

As was proved in [11, 12], the knowledge of Λ_λ permits formulating the following Dyson-type equation for the one-particle Green's function:

$$G_\lambda(k) = \frac{\Lambda_\lambda(k)}{1 - \lambda\epsilon(\mathbf{k})\Lambda_\lambda(k)}. \quad (11)$$

Here, k stands for $(\mathbf{k}, i\omega_n)$ with odd Matsubara frequencies. It follows from (10) and (11) that

$$\widetilde{T}_\lambda(k) = \lambda T_\lambda(k), \\ T_\lambda(k) = \frac{\epsilon(\mathbf{k})}{1 - \lambda\epsilon(\mathbf{k})\Lambda_\lambda(k)}. \quad (12)$$

Equation (12) has the form of a Dyson equation for the tunneling Green's function, and the role of the mass operator Σ_λ is played by the correlation function times the auxiliary constant λ:

$$\Sigma_\lambda(k) = \lambda\Lambda_\lambda(k). \quad (13)$$

In the Hubbard-I approximation, we neglect the correlation function $Z_\lambda(k)$ and consider $\Lambda_\lambda(k)$ equal to the zeroth-order Green's function $G^0(k)$. In this approximation,

$$G_\lambda^{\mathrm{I}}(k) = \frac{G^0(k)}{1 - \lambda\epsilon(\mathbf{k})G^0(k)}$$

which describes two Hubbard energy subbands separated from each other for $U \neq 0$, which cannot describe the Mott–Hubbard transition.

3. THERMODYNAMIC POTENTIAL DIAGRAMS

The thermodynamic potential of the system is determined by the connected part of the mean value of the evolution operator [11, 12]

$$F = F_0 - \frac{1}{\beta}\langle U(\beta)\rangle_0^c. \quad (14)$$

From the beginning, we consider a more general quantity

$$F(\lambda) = F_0 - \frac{1}{\beta}\langle U_\lambda(\beta)\rangle_0^c, \quad (15)$$

and set $\lambda = 1$ at the final stage.

The first-order diagrams for $\langle U_\lambda(\beta)\rangle_0^c$ obtained using the perturbation theory are shown in Fig. 3. To understand these diagram contributions better, we examine the expression

$$\sum_{x,x'} G_\lambda(x|x')\lambda t(\mathbf{x}' - \mathbf{x})\delta(\tau - \tau' - 0^+)\delta_{\sigma\sigma'} = \\ = -\beta\sum_{\mathbf{x},\mathbf{x}'}\sum_{\sigma} G_{\lambda\sigma}(\mathbf{x} - \mathbf{x}'| - 0^+)\lambda t(\mathbf{x}' - \mathbf{x}) = \\ = -\lambda\sum_{\mathbf{k},\sigma}\sum_{\omega_n}\epsilon(\mathbf{k})G_{\lambda\sigma}(\mathbf{k}|i\omega_n)\exp(i\omega_n 0^+), \quad (16)$$
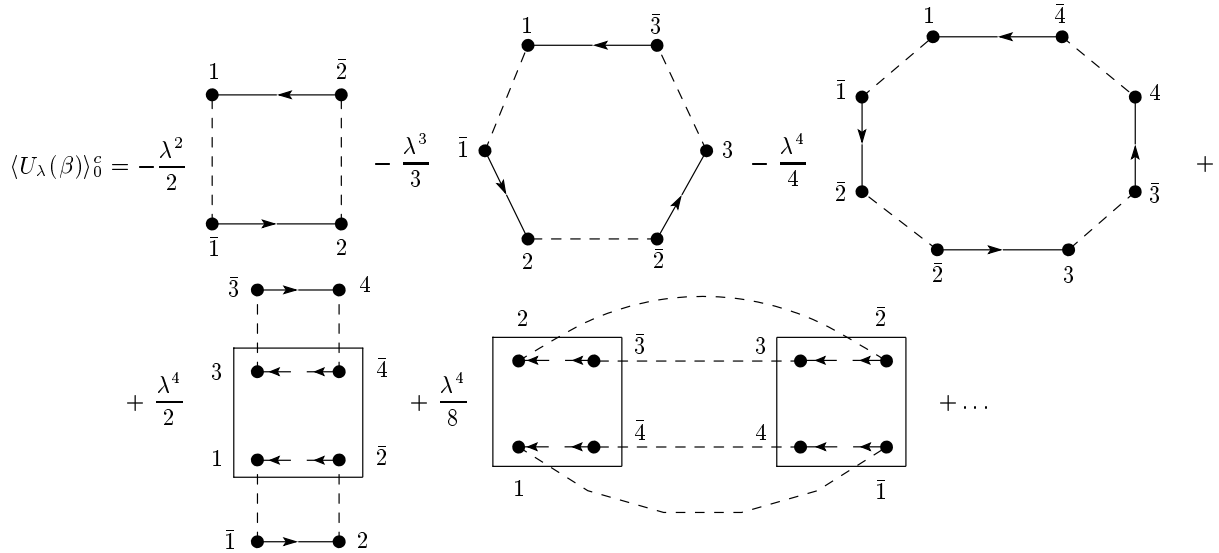
Fig. 3. The first four orders of the perturbation theory for $\langle U_\lambda(\beta)\rangle_0^c$

where summation and integration over repeated indices is assumed and we have integrated with respect to time.

In terms of diagrams, Eq. (16) implies the procedure of locking the external lines of the G_λ propagator diagrams shown in Fig. 1 with the tunneling matrix element $t(\mathbf{x}' - \mathbf{x})$, which yields diagrams without external lines similar to those for $\langle U_\lambda(\beta)\rangle_0^c$ shown in Fig. 3. These two series of diagrams differ by the coefficients in front of them.

In expression (16), the coefficients $1/n$ before each diagram, where n is the order of the perturbation theory, are absent. These coefficients are present in Fig. 3. To restore these $1/n$ coefficients in (16) and obtain the coincidence with the $\langle U_\lambda(\beta)\rangle_0^c$ series, it is enough to integrate (16) with respect to λ, which yields

$$-\sum_{\mathbf{x},\mathbf{x}'}\sum_\sigma \beta \int d\lambda\, t(\mathbf{x}' - \mathbf{x}) G_{\lambda\sigma}(\mathbf{x} - \mathbf{x}' \,|\, -0^+). \quad (17)$$

Expression (17) displayed in the diagram representation exactly coincides with the mean value of the evolution operator:

$$\langle U_\lambda(\beta)\rangle_0^c = -\sum_{\mathbf{x},\mathbf{x}'} \beta t(\mathbf{x}' - \mathbf{x}) \times$$

$$\times \int_0^\lambda d\lambda'\, G_{\lambda'\sigma}(\mathbf{x} - \mathbf{x}' \,|\, -0^+). \quad (18)$$

In the Fourier representation, we have

$$\langle U_\lambda(\beta)\rangle_0^c = -\int_0^\lambda d\lambda' \times$$

$$\times \sum_{\mathbf{k},\sigma,\omega_n} \epsilon(\mathbf{k}) G_{\lambda'\sigma}(\mathbf{k} \,|\, i\omega_n) \exp(i\omega_n 0^+). \quad (19)$$

It follows from (15) and (19) that

$$F(\lambda) = F_0 + \int_0^\lambda d\lambda' \sum_{\mathbf{k},\sigma} \frac{1}{\beta} \times$$

$$\times \sum_{\omega_n} \epsilon(\mathbf{k}) G_{\lambda'\sigma}(\mathbf{k} \,|\, i\omega_n) \exp(i\omega_n 0^+). \quad (20)$$

Using definition (14), Eq. (20) can be written as

$$F(\lambda) = F_0 + \int_0^\lambda \frac{d\lambda'}{\lambda'} \sum_{\mathbf{k},\sigma} \frac{1}{\beta} \times$$

$$\times \sum_{\omega_n} T_{\lambda'}(k) \Sigma_{\lambda'}(k) \exp(i\omega_n 0^+), \quad (21)$$

whence

$$\lambda \frac{F(\lambda)}{d\lambda} = \sum_{\mathbf{k},\sigma} \frac{1}{\beta} \sum_{\omega_n} T_\lambda(k) \Sigma_\lambda(k) \exp(i\omega_n 0^+) =$$

$$= \frac{1}{\beta} \operatorname{Tr}(T_\lambda \Sigma_\lambda). \quad (22)$$

To obtain a full system of equations, we add the definition of the chemical potential to (21),

$$N_e = \sum_{\mathbf{k},\sigma} \frac{1}{\beta} \sum_{\omega_n} G_\sigma(\mathbf{k} \,|\, i\omega_n) \exp(i\omega_n 0^+), \quad (23)$$

$$Y'(\lambda) = -\frac{1}{\beta}\sum_{\mathbf{k},\sigma}\sum_{\omega_n}\left\{\lambda \quad - \frac{\lambda^2}{2} \quad - \frac{\lambda^3}{6} \quad - \right.$$

$$\left. - \frac{\lambda^4}{24} \quad - \frac{\lambda^4}{8} \quad + \dots \right\}.$$
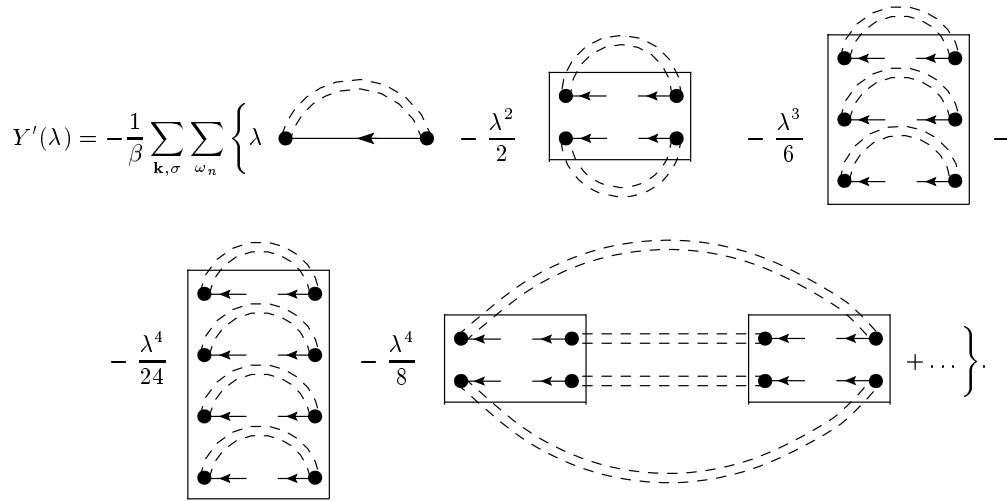
Fig. 4. The simplest skeleton diagrams for the functional $Y'(\lambda)$. Double dashed lines are the tunneling functions $T_\lambda(k)$

where N_e is the number of electrons.

Equation (20) establishes the relation between the thermodynamic potential and the renormalized one-particle propagator. This last quantity depends on the auxiliary parameter λ, and Eq. (20) contains an additional integration over it, which makes this equation inconvenient.

We obtain a more convenient equation for the thermodynamic potential without such an integration over λ. For this, we introduce the special functional [15]

$$Y(\lambda) = Y_1(\lambda) + Y'(\lambda), \tag{24}$$

where

$$Y_1(\lambda) = -\frac{1}{\beta}\sum_{\mathbf{k},\sigma,\omega_n}[\ln(\epsilon(\mathbf{k})\lambda\Lambda_\lambda(k) - 1) +$$
$$+ T_\lambda(k)\lambda\Lambda_\lambda(k)]\exp(i\omega_n 0^+), \tag{25}$$

and $Y'(\lambda)$ is constructed from skeleton diagrams without external lines as shown in Fig. 4.

Our observation about two kinds of skeleton diagrams for the $\Lambda(k)$ function can be repeated in relation to the vacuum skeleton diagrams in Fig. 4.

The dependence on λ in the functional $Y'(\lambda)$ is twofold: through the dependence of the renormalized Green's function $G_\lambda, T_\lambda, \Lambda_\lambda$, and Σ_λ and through the explicit factors λ^n in front of each diagram of $Y'(\lambda)$.

Using the above definitions, we can prove the equations

$$\frac{\delta\beta Y_1(\lambda)}{\delta T_\lambda(k)} = -\lambda\Lambda_\lambda(k) = -\Sigma_\lambda(k),$$
$$\frac{\delta\beta Y'(\lambda)}{\delta T_\lambda(k)} = \lambda\Lambda_\lambda(k) = \Sigma_\lambda(k). \tag{26}$$

As a result, we obtain the stationarity property

$$\frac{\delta\beta Y(\lambda)}{\delta T_\lambda(k)} = 0. \tag{27}$$

Using definition (13) of the mass operator $\Sigma_\lambda(k)$, we can rewrite the functional $Y_1(\lambda)$ in the form

$$Y_1(\lambda) = -\frac{1}{\beta}\sum_{\mathbf{k},\sigma}\sum_{\omega_n}[\ln(\epsilon(\mathbf{k})\Sigma_\lambda(k) - 1) +$$
$$+ T_\lambda(k)\Sigma_\lambda(k)]\exp(i\omega_n 0^+), \tag{28}$$

and prove the second form of the stationarity property

$$\frac{\delta Y(\lambda)}{\delta\Sigma_\lambda(k)} = 0 \tag{29}$$

if we take the Dyson equation for the tunneling function $T_\lambda(k)$ into account.

We now discuss the derivative of the functional $Y(\lambda)$ with respect to λ. Using stationarity property (29), we obtain

$$\frac{dY(\lambda)}{d\lambda} = \sum_k \frac{\delta Y(\lambda)}{\delta\Sigma_\lambda(k)}\frac{\delta\Sigma_\lambda(k)}{\delta\lambda} + \frac{\partial Y(\lambda)}{\partial\lambda}\bigg|_{\Sigma_\lambda} =$$
$$= \frac{\partial Y'(\lambda)}{\partial\lambda}\bigg|_{\Sigma_\lambda} \tag{30}$$

because $Y_1(\lambda)$ in (28) has no explicit dependence on λ.

Using Fig. 4 for $Y'(\lambda)$ and the definition of Λ_λ in Fig. 2, it is easy to establish the property

$$\lambda \frac{\partial Y'(\lambda)}{\partial \lambda}\bigg|_{\Sigma_\lambda} = \frac{1}{\beta} \sum_{\mathbf{k},\sigma} \sum_{\omega_n} T_\lambda(k)\lambda\Lambda_\lambda(k)\exp(i\omega_n 0^+) =$$
$$= \frac{1}{\beta}\operatorname{Tr}(T_\lambda \Lambda_\lambda). \quad (31)$$

It therefore follows from (30) and (31) that

$$\lambda \frac{dY(\lambda)}{d\lambda} = \frac{1}{\beta}\sum_{\mathbf{k},\sigma}\sum_{\omega_n} T_\lambda(k)\Sigma_\lambda(k) = \frac{1}{\beta}\operatorname{Tr}(T_\lambda \Sigma_\lambda). \quad (32)$$

From Eqs. (22) and (32), we have

$$\lambda \frac{dF(\lambda)}{d\lambda} = \lambda \frac{dY(\lambda)}{d\lambda}, \quad (33)$$

and hence

$$F(\lambda) = Y(\lambda) + \text{const.} \quad (34)$$

Because the perturbation is absent for $\lambda = 0$ and $F(0) = F_0$ and $Y(0) = 0$, we have

$$F(\lambda) = Y(\lambda) + F_0. \quad (35)$$

We can now set $\lambda = 1$ to obtain

$$F(1) = Y(1) + F_0 \quad (36)$$

with the stationarity property

$$\frac{\delta F}{\delta \Sigma} = 0. \quad (37)$$

4. CONCLUSIONS

We have developed the diagram theory proposed for the Hubbard model many years ago, and introduced the notion of the renormalized tunneling Green's function T in addition to those known previously. We have defined the correlation function Λ and the mass operator Σ for the tunneling function, and have established Dyson equations for them. The mass operator was found in (13) to be equal to the correlation function for $\lambda = 1$.

We have obtained a diagram representation of the correlation function in terms of the skeleton diagrams that contain the many-particle irreducible Green's functions $G_{2n}^{(0)ir}$ with all possible values of n (the perturbation theory order) and the renormalized tunneling Green's functions.

We have established a relation between renormalized values of the thermodynamic potential and the one-particle Green's function. This last function has an additional dependence on the auxiliary constant λ and must be integrated over it. We have shown that it is possible to avoid such an integration over λ and to introduce the special functional $Y(\lambda)$ constructed from skeleton diagrams. We have proved the stationarity property of this functional and found its relation to the stationarity of the thermodynamic potential with respect to a variation of the mass operator or the full tunneling function. This theorem is a generalization of the known Luttinger and Ward theorem [15] proved for weakly correlated systems to the case of strongly correlated systems described by the Hubbard model.

As regards the diagrams for the correlation function Λ in Fig. 2 and for the functional Y' in Fig. 4, we emphasize that a part of the skeleton diagrams are local, and they are the only ones associated with the dynamical mean field theory. The other diagrams are nonlocal, contain space and time fluctuations, and are omitted in this theory. The generalization of the dynamical mean field theory is related to taking these space fluctuations into account together with time fluctuations.

REFERENCES

1. J. Hubbard, Proc. Roy. Soc. London A **276**, 238 (1963), **277**, 237 (1964), **281**, 401 (1964).

2. P. Fulde, *Electron Correlations in Molecules and Solids*, Springer-Verlag, Berlin (1993).

3. A. C. Hewson, *The Kondo Problem to Heavy Fermions*, Cambridge Univ. Press, Cambridge, England (1993).

4. A. Georges, G. Kotliar, W. Krauth, and M. J. Rozenberg, Rev. Mod. Phys. **8**, 13 (1996).

5. H. Matsumoto and F. Mancini, Phys. Rev. B **55**, 2095 (1997).

6. A. Avella, F. Mancini, and R. Munzner, Phys. Rev. B **63**, 245117 (2001).

7. G. Kotliar and D. Vollhardt, Physics Today **57**, 53 (2004).

8. P. M. Slobodyan and I. V. Stasyuk, Teor. Mat. Fiz. **19**, 423 (1974); Preprint 73-136R (in Russian), Institute of Theoretical Physics, Ukranian SSR Academy of Sciences, Kiev (1973).

9. R. O. Zaitsev, Zh. Eksp. Teor. Fiz. **68**, 207 (1974); Preprint IAE-2378 (in Russian), Institute of Atomic Energy, Moskow (1974).

10. Yu. A. Izyumov, F. L. Kassan-Ogly, and Y. M. Skryabin, *Theory of Statistical Mechanics of Magnito-oriented Systems*, Nauka, Moskow (1987).

11. M. I. Vladimir and V. A. Moskalenko, Teor. Mat. Fiz. **82**, 428 (1990).

12. S. I. Vakaru, M. I. Vladimir, and V. A. Moskalenko, Teor. Mat. Fiz. **85**, 248 (1990).

13. N. N. Bogoliubov and V. A. Moskalenko, Teor. Mat. Fiz. **86**, 16 (1991); **92**, 182 (1992); Doklady AN SSSR **316**, 1107 (1991); JINR Rapid Comm. **44**, 5 (1990).

14. W. Metzner, Phys. Rev. B **43**, 8549 (1991).

15. J. M. Luttinger and J. C. Ward, Phys. Rev. **118**, 1417 (1960).

16. V. A. Moskalenko, P. Entel, L. A. Dohotaru, and R. Citro, Teor. Mat. Fiz. **159**, 154 (2009); arXiv:0804.1651.